Electronic Supporting Information (ESI)

Exploring Compositional Versatility of Perovskite-Like $Cs_3(Bi,Sb)_2X_9$ (X = Cl, Br, I) Compounds By High-Throughput Experimentation

Oleksandr Stroyuk[1*], Oleksandra Raievska[1], Sachin Kinge[2], Jens Hauch[1,3], Christoph J. Brabec[1,3]

[1]*Forschungszentrum Jülich GmbH, Helmholtz-Institut Erlangen Nürnberg für Erneuerbare Energien (HI ERN), 91058 Erlangen, Germany*
[2]*Materials Engineering Div., Toyota Motors Europe, sachin.kinge@toyota-europe.com*
[3]*Friedrich-Alexander-Universität Erlangen-Nürnberg, Materials for Electronics and Energy Technology (i-MEET), Martensstrasse 7, 91058 Erlangen, Germany*

Authors for correspondence:
[*]Dr. Oleksandr Stroyuk, Forschungszentrum Jülich GmbH, Helmholtz-Institut Erlangen Nürnberg für Erneuerbare Energien (HI ERN), Immerwahrstr. 2, 91058 Erlangen, Germany; *e-mail*: o.stroyuk@fz-juelich.de, alstroyuk@ukr.net.

1 Methods and materials

1.1 Methods of characterization

X-ray diffraction (XRD) patterns were registered using a Panalytical X'pert powder diffractometer with filtered Cu K_α radiation (λ = 1.54178 Å) and an X'Celerator solid-state stripe detector in the Bragg-Brentano geometry in an angle range of 2θ = 5-100° with a step rate of 0.05° per min. The XRD patterns were subjected to a Rietveld refinement procedure using MAUD software (version 2.99) using structural CIF files from the Crystallography Open Database (https://www.crystallography.net/cod/). COD ID numbers for the CIF files used in the refinements are 1011025 (AgI), 2106275 (hexagonal $Cs_3Bi_2I_9$), 2106376 (trigonal $Cs_3Bi_2Br_9$), 5910351 (trigonal $Cs_3Sb_2Cl_9$), 1537138 (trigonal $Cs_3Sb_2Br_9$), 1520793 (trigonal $Cs_3Sb_2I_9$), 4003575 (cubic $Cs_2NaInCl_6$), 7249637 (cubic $Cs_2AgBiCl_6$), and 4131244 (cubic $Cs_2AgBiBr_6$).

Scanning electron microscopy (SEM) imaging and energy-dispersive X-ray spectroscopic (EDX) analysis were performed using a JEOL JSM-7610F Schottky field emission scanning electron microscope operating under 15-20 kV acceleration voltage and equipped with an X-Max 80 mm^2 silicon drift detector (Oxford Instruments) and AZtec nanoanalysis software. EDX spectra were collected for at least four different spots of each sample, and the results were averaged.

Reflectance spectra were recorded using a BlackComet spectrometer (StellarNet Inc.) and a 75 W Xenon lamp (Thorlabs) as an excitation source. The spectra were registered with an optical Y-fiber probe in identical geometry for samples and a scattering reference (ultra-pure $BaSO_4$, Alfa-Aesar). The reflectance spectra were transformed into absorption spectra using the Kubelka-Munk formula and the reference.

1.2 Synthesis of samples

1.2.1 Synthesis of $Cs_3Bi_2(Cl,Br,I)_9$ samples.

On the first step, an 8×6 sample array of identical $Cs_2AgBiCl_6$ (CABC) was prepared using a robotized setup (see more details in 10.1039/D4TC01693A). The CABC synthesis requires two precursors.

Precursor #1 is produced by mixing 5.0 mL aqueous 1.0 M $BiCl_3$ solution containing 4.0 M HCl with 10.0 mL aqueous 12 M (37%) HCl and 25 mL 2-propanol in a 50 mL beaker under intense refluxing. This precursor solution is divided into four 10.0 mL vials and transferred into the vials arranged in an Eppendorf plate (0.8 mL per each of 48 vials), simultaneously by four nozzles of the pipetting robot to minimize evaporation of 2-propanol during the transfer. At that, the plate is kept on a shaking platform under continuous refluxing.

Precursor #2 is produced by mixing 6.0 mL deionized (DI) water with 5.0 mL aqueous 1.0 M $AgNO_3$ solution, followed by 1.25 mL aqueous 25% NH_4OH solution, 3.0 mL aqueous 4.0 M Cs acetate solution, and 25 mL 2-propanol in a 50-mL beaker, all mixings performed under intense magnetic stirring. This precursor solution is divided into four 10.0 mL vials and is transferred into the vials (0.8 mL for each) with the first precursor simultaneously by four nozzles of the pipetting robot to minimize evaporation of 2-propanol during the transfer. At that, the plate is kept on a shaking platform under continuous stirring.

In 5-10 minutes after the precursors transfer, the Eppendorf vials are manually closed with their caps and left without refluxing for 12 h. Afterwards, the vials are centrifuged at 1500 rpm for 2 min, the supernatant is discarded. Then, 1.0 mL 2-propanol is added to each of the vials with precipitates, the solutions are stirred to form homogeneous suspensions, and centrifuged at 1500 rpm for 2 min for purification. The supernatant with side salts and unreacted precursors is discarded, and the purification procedure is repeated once again.

On the second step, the array of 48 CABC samples is subjected to anion exchange with mixtures of NaBr and NaI. The scheme of NaBr/NaI additions is presented below in Table S1. For the anion exchange,

solutions of NaBr+NaI in 2-propanol/water/glycerol mixtures are added to freshly prepared and purified CABC samples. Water is required to enable ionic equilibria in the system, while a 2-propanol-glycerol mixture is used to dissolve NaCl as the product of anion exchange, which is insoluble in pure 2-propanol and contaminates the final products. The 2-propanol/glycerol mixture was prepared by mixing 50 mL of 2-propanol with 25 g of glycerol.

Aqueous NaBr/NaI solutions with different ratios of NaBr and NaI were prepared by using the robotic setup on an auxiliary Eppendorf vial plate by mixing different amounts of aqueous 4.0 M stock solutions of NaBr and NaI as presented in the following tables:

Column	1	2	3	4	5	6	7	8
4.0 M NaI	0ml 0%	0.03ml 20%	0.06ml 40%	0.075ml 50%	0.09ml 60%	0.12ml 80%	0.15ml 100%	0.18ml 120%

Row	A	B	C	D	E	F
4.0 M NaBr	0ml 0%	0.03ml 20%	0.06ml 40%	0.075ml 50%	0.09ml 60%	0.12ml 80%

For the anion exchange, 0.6 mL of 2-propanol/glycerol mixture is first added to each of the CABC samples under refluxing, resulting in the formation of homogeneous suspensions. Then, 0.6 mL of 2-propanol/glycerol as well as calculated volumes of aqueous NaBr/NaI mixtures from the above-described auxiliary plate are added, both under intense refluxing. In 10 min after NaBr/NaI addition, the vials are closed with the caps, refluxed for ca. 30 min, and then left with no refluxing for 12 h. Afterwards, the samples are subjected to purification with 2-propanol as described above for CABC samples, but with triple repetition of the purification cycle.

On the third step, samples for structural and spectral characterizations were produced. Freshly purified microcrystalline products of anion exchange were then mixed with 0.3 mL 2-propanol and refluxed to achieve the formation of homogeneous suspensions. For each sample, 40 µL was drop-casted on a circular pit of a special plastic Eppendorf plate (for spectral measurements), 1 cm^2 glass substrates (for XRD), or a silicon substrate (for SEM/EDX) and left to dry under natural ventilation. The examples of original suspensions and samples for characterization are presented in Fig. S5.

1.2.2 Synthesis of $Cs_3Bi_2(Br,I)_9$ samples.

On the first step, an array of six identical rows of $Cs_3(Bi,Sb)_2Br_9$ samples were produced (designated as A through F) with the molar Bi and Sb fractions varied from pit 1 to pit 8 as shown in the table:

	1	2	3	4	5	6	7	8
Bi	100%	80%	70%	60%	50%	40%	20%	0
Sb	0%	20%	30%	40%	50%	60%	80%	100%

To produce each of the rows A-F two-precursor synthesis scheme was applied. Eight versions of precursor #1 were produced by mixing 0.2 mL aqueous 1.0 M solution of $BiBr_3$ + $SbBr_3$ (with different Bi/Sb ratios) in 5.0 M HBr with 0.5 mL 2-propanol and 0.2 mL aqueous 8.9 M (48%) HBr. Precursor #2 was prepared by mixing 0.075 mL DI water, 0.075 mL of aqueous 4.0 M Cs acetate, and 0.5 mL 2-propanol.

Then, 0.9 mL of each of the eight versions of the precursor #1 was transferred into the corresponding vials 1 through 8 of each of the rows A through F, and 0.65 mL of the second precursor was added to each of 48 vials under intense refluxing.

After mixing the precursors, the vials were left refluxing for 5 min, closed with corresponding caps, and left for 12 h with no refluxing. Afterwards, the suspensions were subjected to centrifugation at 1500 rpm for 2 min and two cycles of purification using 1.0 mL 2-propanol additions, as described above for the synthesis of CABC.

On the next step, the freshly prepared $Cs_3(Bi,Sb)_2Br_9$ (CBS-B) samples were subjected to anion exchange with different amounts of NaI. In contrast to the anion exchanges with chloride precursors. In this case, 2-propanol/water mixtures were used without additions of glycerol.

For anion exchange, 0.5 mL 2-propanol was first added to each of the CBS-B samples, and the samples were refluxed to form homogeneous suspensions. Then, NaI solution in 2-propanol/water mixtures was added at intense refluxing. Table S6 illustrates the nominal contents of Bi and NaI in each of 48 samples. The scheme of additions is as follows:

row A: 1.0 mL pure 2-propanol (0% NaI);
row B: 1.0 mL 2-propanol and 0.030 mL aqueous 4.0 M NaI (13% NaI with respect to the stoichiometric amount necessary for complete substitution of bromide with iodide);
row C: 1.0 mL 2-propanol and 0.075 mL aqueous 4.0 M NaI (33% NaI);
row D: 1.0 mL 2-propanol and 0.150 mL aqueous 4.0 M NaI (66% NaI);
row E: 1.0 mL 2-propanol and 0.180 mL aqueous 4.0 M NaI (80% NaI);
row F: 1.0 mL 2-propanol and 0.225 mL aqueous 4.0 M NaI (100% NaI).

After NaI additions, the samples are left under intense refluxing for 15 min and then closed with corresponding caps and left unrefluxed for 12 h. Then, the mixtures are subjected to centrifugation at 1500 rpm for 2 min and three cycles of purification of the precipitates with 1.0 mL 2-propanol as described above for CABC and CBS-B.

The freshly purified samples were converted into homogeneous suspensions by the addition of 0.3 mL 2-propanol and refluxing, and 40 µL of each sample was drop-casted on plastic, glass, or silicon substrates (1.0 cm^2) for characterizations, similar to the above-discussed CB-CBI samples.

We note that the ambient temperature and relative humidity in the lab were controlled continuously and set for all synthetic procedures at 22- 23 °C and 55-60%, respectively. The reproducibility of the synthesis was tested for three batches of bromide double salts that were expected to be most sensitive to moisture, yielding identical results for all three batches.

2 Tables

Table S1. Nominal amounts of NaBr and NaI in the sample array $Cs_3Bi_2X_9$, X = Cl+Br+I

	1	2	3	4	5	6	7	8
A	NaI 0 NaBr 0	NaI 20% NaBr 0	NaI 40% NaBr 0	NaI 50% NaBr 0	NaI 60% NaBr 0	NaI 80% NaBr 0	NaI 100% NaBr 0	NaI 120% NaBr 0
B	NaI 0 NaBr 20%	NaI 20% NaBr 20%	NaI 40% NaBr 20%	NaI 50% NaBr 20%	NaI 60% NaBr 20%	NaI 80% NaBr 20%	NaI 100% NaBr 20%	NaI 120% NaBr 20%
C	NaI 0 NaBr 40%	NaI 20% NaBr 40%	NaI 40% NaBr 40%	NaI 50% NaBr 40%	NaI 60% NaBr 40%	NaI 80% NaBr 40%	NaI 100% NaBr 40%	NaI 120% NaBr 40%
D	NaI 0 NaBr 50%	NaI 20% NaBr 50%	NaI 40% NaBr 50%	NaI 50% NaBr 50%	NaI 60% NaBr 50%	NaI 80% NaBr 50%	NaI 100% NaBr 50%	NaI 120% NaBr 50%
E	NaI 0 NaBr 60%	NaI 20% NaBr 60%	NaI 40% NaBr 60%	NaI 50% NaBr 60%	NaI 60% NaBr 60%	NaI 80% NaBr 60%	NaI 100% NaBr 60%	NaI 120% NaBr 60%
F	NaI 0 NaBr 80%	NaI 20% NaBr 80%	NaI 40% NaBr 80%	NaI 50% NaBr 80%	NaI 60% NaBr 80%	NaI 80% NaBr 80%	NaI 100% NaBr 80%	NaI 120% NaBr 80%

Table S2. Summary of sample characteristics in the $Cs_3Bi_2(Cl,Br,I)_9$ array: composition, phase fractions, elementary cell volume, $V_{CB\text{-}CBI}$, and bandgap, E_g, of the CBS-CBI phase

Sample ID	Actual composition (EDX)					Phase fractions				$V_{CB\text{-}CBI}$ (Å^3)	E_g, eV
	Cs/Bi	X/Bi	Cl/X	Br/X	I/X	CB-CBI	CABCB	AgI	CB-I		
A1	1.9	5.6	1.00	0	0	0	100	0	0	-	-
A2	1.9	5.6	0.92	0	0.08	0	97	0	3	-	-
A3	1.9	5.7	0.76	0	0.24	0	69	0	31	-	-
A4	1.9	5.8	0.67	0	0.33	0	60	0	40	-	-
A5	1.9	5.8	0.65	0	0.35	0	52	0	48	-	-
A6	1.9	5.8	0.53	0	0.47	0	24	0	76	-	-
A7	2	5.9	0.38	0	0.62	0	15	0	85	-	-
A8	1.6	5.4	0.13	0	0.87	0	9	0	91	-	-
B1	1.9	5.8	0.89	0.11	0	0	100	0	0	-	-
B2	1.9	5.6	0.75	0.09	0.16	11	64	9	16	-	-
B3	1.7	5.6	0.61	0.12	0.27	27	60	15	14	-	-
B4	1.7	5.4	0.56	0.09	0.35	35	45	6	14	-	-
B5	1.8	5.5	0.45	0.09	0.46	73	10	5	12	-	-
B6	1.9	5.6	0.35	0.05	0.60	40	10	9	42	-	-
B7	1.8	5.6	0.16	0.05	0.79	10	0	5	85	-	-
B8	1.7	5.4	0.03	0.03	0.94	0	0	5	95	-	-
C1	2.0	5.9	0.76	0.24	0	0	100	0	0	-	-
C2	1.8	5.6	0.68	0.18	0.14	50	40	10	0	-	-
C3	1.8	5.7	0.46	0.23	0.31	**79**	16	5	0	560.1	2.25
C4	1.6	5.5	0.41	0.21	0.38	**88**	9	3	0	576.8	2.21
C5	1.5	4.9	0.25	0.25	0.50	**88**	7	5	0	591.8	2.14
C6	1.6	5.1	0.13	0.20	0.67	**96**	0	4	0	611.2	2.07
C7	1.5	4.8	0.05	0.14	0.81	55	0	4	41	-	-
C8	1.4	4.7	0.03	0.07	0.90	3	0	3	94	-	-
D1	2.1	5.8	0.66	0.34	0	0	100	0	0	-	-
D2	1.7	5.8	0.62	0.26	0.12	**82**	0	18	0	557.2	2.48
D3	1.7	5.0	0.44	0.27	0.29	**94**	0	6	0	561.9	2.27
D4	1.6	5.2	0.33	0.30	0.37	**95**	0	5	0	577.8	2.23
D5	1.7	5.1	0.23	0.28	0.49	**96**	0	4	0	597.2	2.16
D6	1.5	5.0	0.13	0.28	0.59	**97**	0	3	0	611.3	2.09
D7	1.5	5.1	0.08	0.18	0.74	69	0	3	28	-	-
D8	1.5	5.2	0.03	0.07	0.90	2	0	3	95	-	-
E1	2.1	5.9	0.61	0.39	0	0	100	0	0	-	-
E2	1.7	5.8	0.53	0.33	0.14	**90**	0	10	0	558.9	2.47
E3	1.7	5.2	0.34	0.34	0.32	**93**	0	7	0	563.3	2.28
E4	1.6	5.2	0.28	0.33	0.39	**95**	0	5	0	575.1	2.23
E5	1.7	5.3	0.20	0.28	0.52	**96**	0	4	0	596.8	2.17
E6	1.6	5.3	0.11	0.25	0.64	**96**	0	4	0	601.1	2.09
E7	1.6	5.4	0.07	0.21	0.72	**75**	0	3	22	621.8	2.04
E8	1.5	5.4	0.05	0.10	0.85	29	0	3	68	-	-
F1	1.9	5.9	0.51	0.49	0	0	100	0	0	-	-
F2	1.6	5.2	0.40	0.47	0.13	**90**	0	10	0	554.9	2.48
F3	1.5	5.3	0.23	0.42	0.35	**95**	0	5	0	562.2	2.29
F4	1.5	5.3	0.18	0.37	0.45	**95**	0	5	0	578.8	2.27
F5	1.6	4.8	0.14	0.35	0.51	**94**	0	6	0	597.1	2.19
F6	1.5	5.0	0.07	0.34	0.59	**95**	0	5	0	613.7	2.09
F7	1.5	4.6	0.06	0.26	0.68	**93**	0	3	4	624.3	2.05
F8	1.5	4.6	0.04	0.12	0.84	35	0	4	61	-	-

Table S3. Summary of sample characteristics in the $Cs_3(Bi_xSb_{1-x})_2Cl_9$ array: composition, elementary cell volume, V_{CBS-C}, and bandgap, E_g, of the CBS-C phase

Nominal Bi	Actual Bi	Cl/(Bi+Sb)	Cs/(Bi+Sb)	V_{CBS-C} (Å^3)	E_g (eV)
0	0	4.4	1.7	459.6	2.96
0.05	0.07	4.6	1.7	460.2	2.88
0.10	0.15	4.5	1.7	461.1	2.85
0.25	0.26	4.6	1.8	462.3	2.83
0.50	0.52	4.7	1.9	465.8	2.83
0.75	0.76	4.7	1.9	467.9	2.88
0.90	0.87	4.8	2.0	470.3	2.95
1.00	1.00	5.3	2.3	470.8	3.10

Notes: The measurement accuracies are 0.02, 0.10, 0.10, 0.1, and 0.01 for the actual Bi fraction, Cl/(Bi+Sb), Cs/(Bi+Sb), V_c, and E_g, respectively.

Table S4. Summary of sample characteristics in the $Cs_3(Bi,Sb)_2X_9$ array, X = Cl+Br: composition, elementary cell volume, V_{CBS-CB}, and bandgap, E_g, of the CBS-CB phase

Nominal Bi	Actual Bi	Cl/X	X/(Bi+Sb)	Cs/(Bi+Sb)	V_{CBS-CB} (Å^3)	E_g (eV)
0	0	0.30	4.2	1.4	511.1	2.58
0.05	0.05	0.28	4.6	1.6	511.9	2.54
0.10	0.12	0.25	4.3	1.5	513.3	2.50
0.25	0.24	0.28	3.9	1.5	514.2	2.48
0.50	0.51	0.26	4.2	1.5	516.8	2.47
0.75	0.76	0.27	4.1	1.6	520.9	2.54
0.90	0.92	0.26	4.4	1.5	523.2	2.62
1.00	1.00	0.23	4.3	1.5	523.9	2.67

Notes: The measurement accuracies are 0.02, 0.10, 0.10, 0.1, 0.1, and 0.01 for the actual Bi fraction, Cl/X, X/(Bi+Sb), Cs/(Bi+Sb), V_c, and E_g, respectively.

Table S5. Summary of sample characteristics in the $Cs_3(Bi_xSb_{1-x})_2I_9$ array: composition, elementary cell volume, V_{CBS-I}, and bandgap, E_g, of the CBS-I phase

Nominal Bi	Actual Bi	I/(Bi+Sb)	Cs/(Bi+Sb)	V_{CBS-I} (Å^3)	E_g (eV)
0	0	4.6	1.5	1259.1	2.03
0.05	0.05	4.3	1.4	1261.9	2.01
0.10	0.12	4.6	1.4	1263.7	1.98
0.25	0.22	4.6	1.6	1267.8	1.97
0.50	0.51	4.7	1.7	1279.2	2.01
0.75	0.76	4.8	1.6	1290.8	2.06
0.90	0.93	4.6	1.7	1298.3	2.09
1.00	1.00	4.8	1.7	1302.3	2.11

Notes: The measurement accuracies are 0.02, 0.10, 0.10, 0.1, and 0.01 for the actual Bi fraction, I/(Bi+Sb), Cs/(Bi+Sb), V_c, and E_g, respectively.

Table S6. Nominal Bi contents and added NaI for different samples in $Cs_3(Bi,Sb)_2Br_9$ array

	1	2	3	4	5	6	7	8
A	Bi 100% NaI 0	Bi 80% NaI 0	Bi 70% NaI 0	Bi 60% NaI 0	Bi 50% NaI 0	Bi 40% NaI 0	Bi 20% NaI 0	Sb 100% NaI 0
B	Bi 100% NaI 13%	Bi 80% NaI 13%	Bi 70% NaI 13%	Bi 60% NaI 13%	Bi 50% NaI 13%	Bi 40% NaI 13%	Bi 20% NaI 13%	Sb 100% NaI 13%
C	Bi 100% NaI 33%	Bi 80% NaI 33%	Bi 70% NaI 33%	Bi 60% NaI 33%	Bi 50% NaI 33%	Bi 40% NaI 33%	Bi 20% NaI 33%	Sb 100% NaI 33%
D	Bi 100% NaI 66%	Bi 80% NaI 66%	Bi 70% NaI 66%	Bi 60% NaI 66%	Bi 50% NaI 66%	Bi 40% NaI 66%	Bi 20% NaI 66%	Sb 100% NaI 66%
E	Bi 100% NaI 80%	Bi 80% NaI 80%	Bi 70% NaI 80%	Bi 60% NaI 80%	Bi 50% NaI 80%	Bi 40% NaI 80%	Bi 20% NaI 80%	Sb 100% NaI 80%
F	Bi 100% NaI 100%	Bi 80% NaI 100%	Bi 70% NaI 100%	Bi 60% NaI 100%	Bi 50% NaI 100%	Bi 40% NaI 100%	Bi 20% NaI 100%	Sb 100% NaI 100%

Table S7. Summary of sample characteristics in the $Cs_3(Bi_xSb_{1-x})_2X_9$ array, X = Br+I: stoichiometry, fractions of tetragonal CBS-BI and hexagonal CBS-I phases, f_{trig} and f_{hex}, volumes of elementary CBS-BI lattice cell for tetragonal and hexagonal modifications, V_{trig}, and V_{hex}, bandgaps E_g of tetragonal CBS-BI phase

Sample ID	Bi fraction		X/ (Bi+Sb)	Cs/ (Bi+Sb)	Br/X	f_{trig}, %	V_{trig}, Å^3	f_{hex} %	V_{hex}, Å^3	E_g, eV
	nom.	actual								
B1	1.00	1.00	4.5	1.4	0.84	100	568.6	-	-	2.20
B2	0.80	0.80	4.2	1.5	0.84	100	560.9	-	-	2.15
B3	0.70	0.67	4.3	1.5	0.86	100	553.3	-	-	2.09
B4	0.60	0.60	4.2	1.4	0.84	100	551.9	-	-	2.08
B5	0.50	0.47	4.2	1.5	0.82	100	546.4	-	-	2.04
B6	0.40	0.40	4.6	1.5	0.83	100	545.0	-	-	2.04
B7	0.20	0.18	4.4	1.4	0.85	100	538.5	-	-	1.96
B8	0	0	4.3	1.5	0.86	100	492.9	-	-	2.19
C1	1.00	1.00	4.6	1.4	0.62	100	595.5	-	-	2.14
C2	0.80	0.80	4.3	1.4	0.57	100	591.8	-	-	2.12
C3	0.70	0,67	4.2	1.4	0.57	100	590.3	-	-	2.10
C3	0.60	0.60	4.3	1.4	0.62	100	585.7	-	-	2.09
C5	0.50	0.50	4.5	1.4	0.62	100	583.2	-	-	2.09
C6	0.40	0.38	4.3	1.4	0.58	100	582.2	-	-	2.09
C7	0.20	0.20	4.2	1.5	0.62	100	575.4	-	-	2.13
C8	0	0	4.2	1.5	0.65	100	571.1	-	-	2.21
D1	1.00	1.00	4.5	1.6	0.21	100	619.8	-	-	2.07
D2	0.80	0.79	4.3	1.5	0.29	100	621.9	-	-	2.05
D3	0.70	0.69	4.2	1.5	0.25	100	621.2	-	-	2.01
D4	0.60	0.60	4.1	1.4	0.31	100	620.3	-	-	2.00
D5	0.50	0.47	4.1	1.4	0.30	100	623.8	-	-	1.99
D6	0.40	0.40	4.2	1.4	0.32	100	616.5	-	-	1.97
D7	0.20	0.20	4.2	1.4	0.35	100	618.8	-	-	1.96
D8	0	0	4.3	1.4	0.28	100	627.6	-	-	2.00
E1	1.00	1.00	4.5	1.5	0.16	9	644.5	91	1290	2.09
E2	0.80	0.80	4.3	1.4	0.18	21	639.6	79	1287	2.03
E3	0.70	0.69	4.4	1.5	0.13	29	639.6	71	1283	2.00
E4	0.60	0.57	4.4	1.4	0.18	51	636.0	49	1280	1.98
E5	0.50	0.47	4.2	1.4	0.17	54	632.8	46	1276	1.96
E6	0.40	0.40	4.3	1.4	0.17	97	630.5	3	1272	1.95
E7	0.20	0.20	4.1	1.4	0.18	100	629.4	0	-	1.94
E8	0	0	4.2	1.4	0.14	100	629.8	0	-	1.99
F1	1.00	1.00	4.3	1.4	0.06	2	650.2	98	1302	2.08
F2	0.80	0.78	4.2	1.4	0.08	5	645.9	95	1291	2.03
F3	0.70	0.69	4.2	1.4	0.08	12	642.8	88	1290	1.98
F4	0.60	0.59	4.2	1.4	0.06	19	642.0	81	1287	1.96
F5	0.50	0.50	4.1	1.4	0.08	24	640.0	76	1284	1.95
F6	0.40	0.38	4.2	1.4	0.10	38	638.1	62	1279	1.93
F7	0.20	0.19	4.3	1.3	0.06	60	635.5	40	1267	1.92
F8	0	0	4.3	1.4	0.12	97	632.8	3	1265	1.99

Table S8. Summary of spectral parameters extracted from absorption spectra of CB-CBI samples in series E.

Sample ID	E_g (in), eV	E_g (d), eV	ΔE_g, meV	Linear section		L_{in}, meV	L_d, meV	L_{in}/L_d
				indirect	direct			
E2	2.517	2.619	102	2.753 - 2.621	2.819 - 2.678	132	141	0.94
E3	2.287	2.393	106	2.425 - 2.318	2.520 - 2.440	107	80	1.34
E4	2.233	2.315	82	2.370 - 2.306	2.423 - 2.358	64	65	0.98
E5	2.192	2.279	87	2.350 - 2.272	2.381 - 2.310	80	71	1.13
E6	2.101	2.175	74	2.231 - 2.163	2.280 - 2.208	68	72	0.94
E7	2.051	2.121	70	2.180 - 2.112	2.235 - 2.155	68	80	0.85
E8	2.057	2.151	94	2.230 - 2.115	2.307 - 2.186	115	121	0.95

Description of parameters: E_g(in) – indirect bandgap, E_g(d) – direct bandgap, ΔE_g – difference between direct and indirect bandgaps, L_{in} and L_d - lengths of linear sections of absorption slopes along the X-axis for the spectra presented in Tauc coordinates for indirect and direct electron transitions, as well as their ratio L_{in}/L_d.

3 Figures

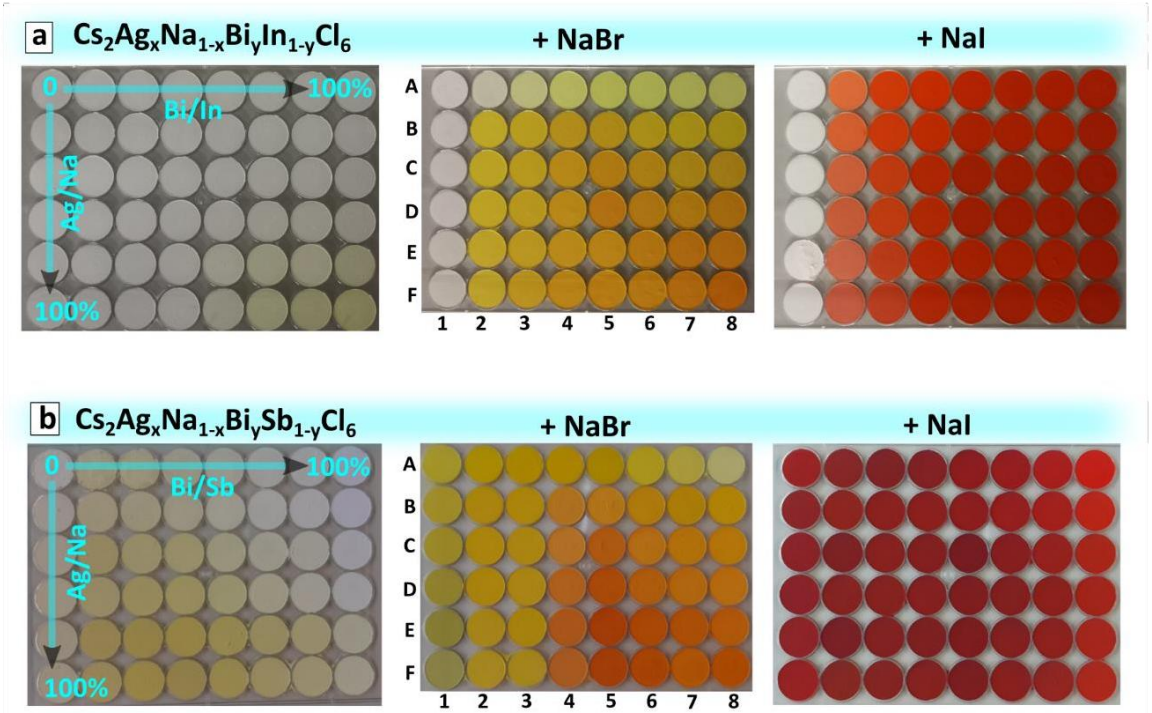

Figure S1. Photographs of sample arrays of original CANBIC ($Cs_2Ag_xNa_{1-x}Bi_yIn_{1-y}Cl_6$) and CANBSC ($Cs_2Ag_xNa_{1-x}Bi_ySb_{1-y}Cl_6$) compounds and the products of their anion exchanges with NaBr and NaI. The silver fraction is 0 (A), 0.1 (B), 0.3 (C), 0.5 (D), 0.8 (E), and 1.0 (F). The bismuth fraction is 0 (1), 0.05 (2), 0.10 (3), 0.25 (4), 0.50 (5), 0.75 (6), 0.90 (7), and 1.00 (8).

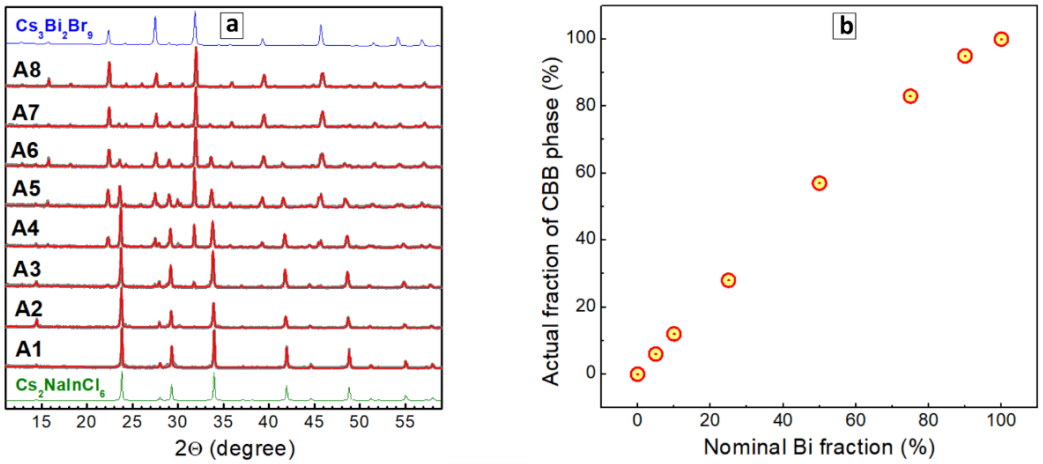

Figure S2. (a) Powder XRD patterns of the products of anion exchange of CNBIC samples (CANBIC plate, series A) with NaBr. Gray lines correspond to experimental data, and red lines show the results of Rietveld refinement. (b) Dependence of CBB fraction on the nominal Bi fraction in original CNBIC perovskites. The content of the CBB phase was evaluated by the Rietveld refinement of the experimental XRD profiles using a combination of CBB and CNIC reference structures.

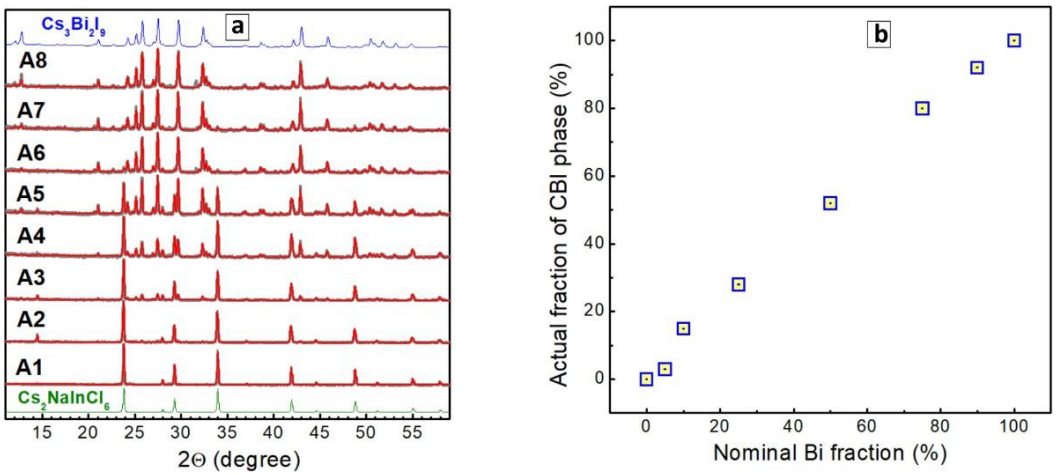

Figure S3. (a) Powder XRD patterns of the products of anion exchange of CNBIC samples (CANBIC plate, series A) with NaI. Gray lines correspond to experimental data, and red lines show the results of Rietveld refinement. (b) Dependence of CBI fraction on the nominal Bi fraction in the original CNBIC perovskites. The content of the CBI phase was evaluated by the Rietveld refinement of the experimental XRD profiles using a combination of CBI and CNIC reference structures.

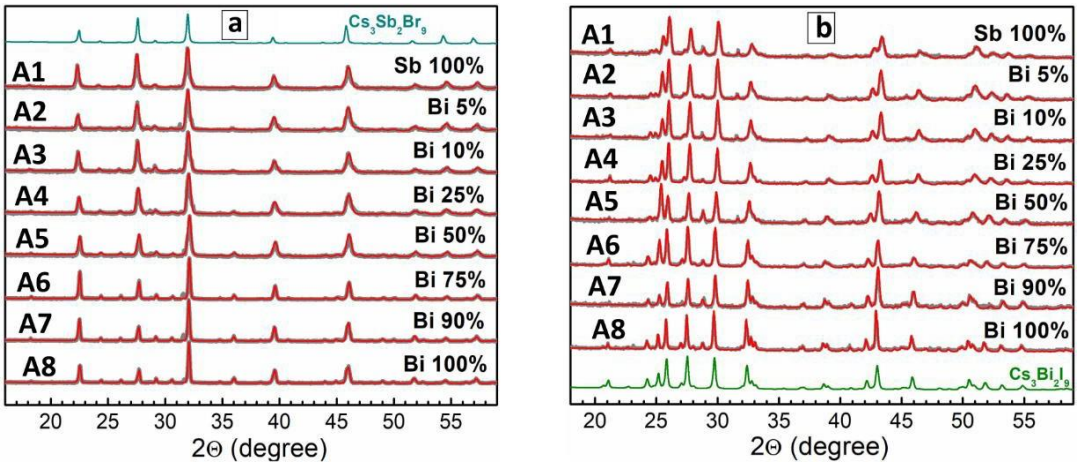

Figure S4. Powder XRD patterns of the products of anion exchange of CANBSC samples in row A with NaBr (a) and NaI (b). Gray lines correspond to experimental data, and red lines show the results of Rietveld refinement.

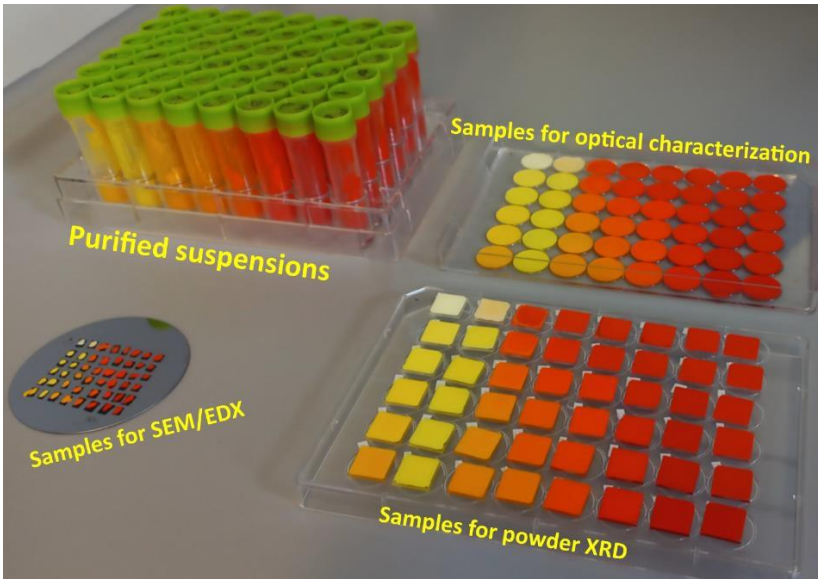

Figure S5. Photograph of a set of anion-exchanged $Cs_3Bi_2X_9$ (X = Cl+Br+I) samples produced by high-throughput experimentation.

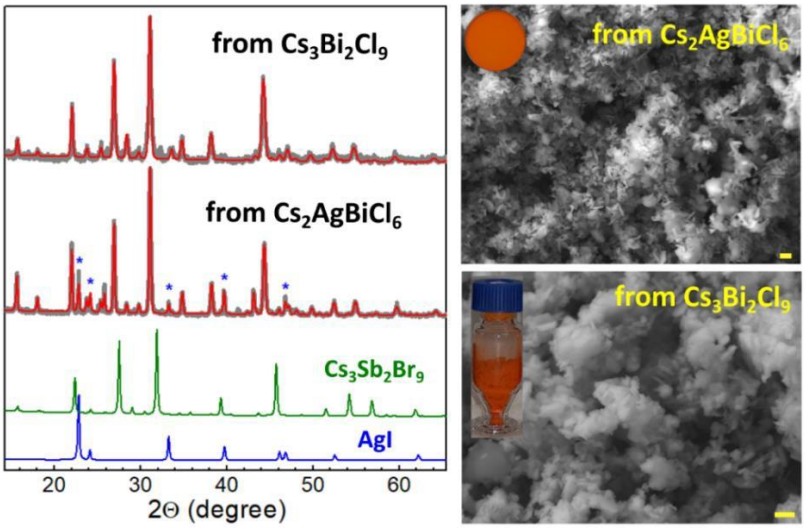

Figure S6. Powder XRD patterns (left panel) and SEM images (right panel) of anion-exchange products collected after the interaction of $Cs_3Bi_2Cl_9$ and $Cs_2AgBiCl_6$ with a NaBr/NaI mixture (1:1) and a single-step purification (to eliminate excesses of NaBr and NaI). Left panel: Gray lines show experimental data, red lines correspond to Rietveld refinement performed using CIF of isostructural trigonal $Cs_3Sb_2Br_6$ double salt. Right panel: the scale bar is 1 μm.

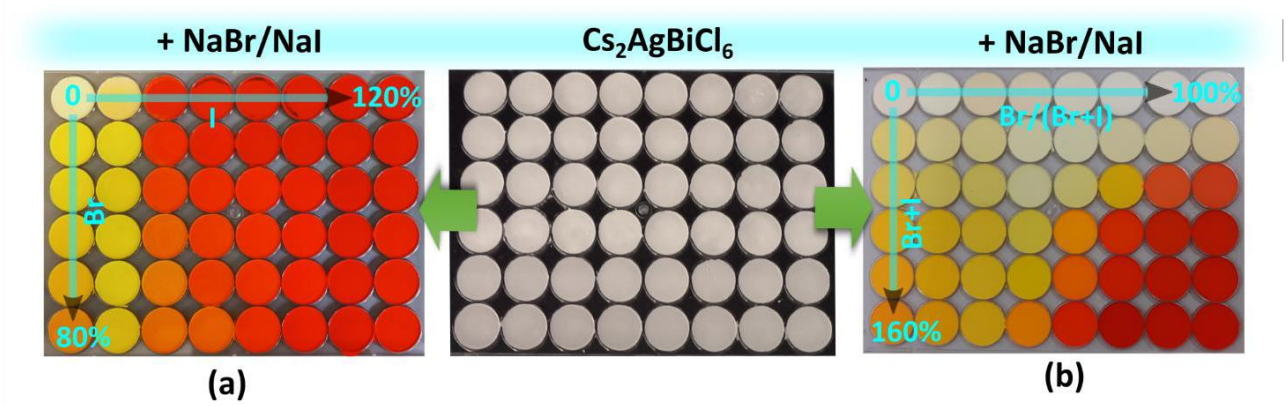

Figure S7. Two modes of NaBr/NaI variations: (a) independent increase of NaI and NaBr amounts along different axes and (b) variation of the NaBr/NaI ratio along the X-axis with simultaneous increase of the total NaBr+NaI amount along the Y-axis.

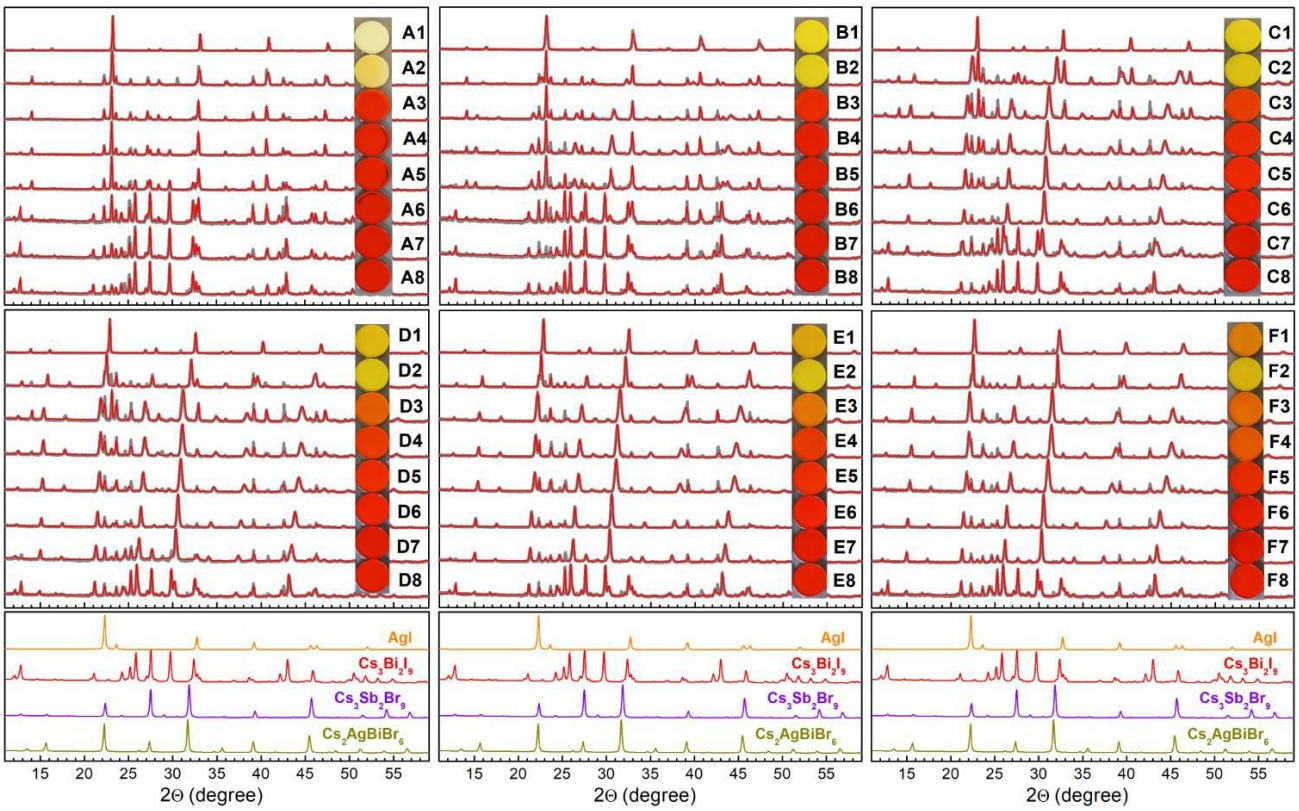

Figure S8. The collection of powder XRD patterns for the plate presented in Fig. S7a. Gray lines are experimental data, red lines represent Rietveld refinement, and lower panels show reference patterns used for the Rietveld refinement.

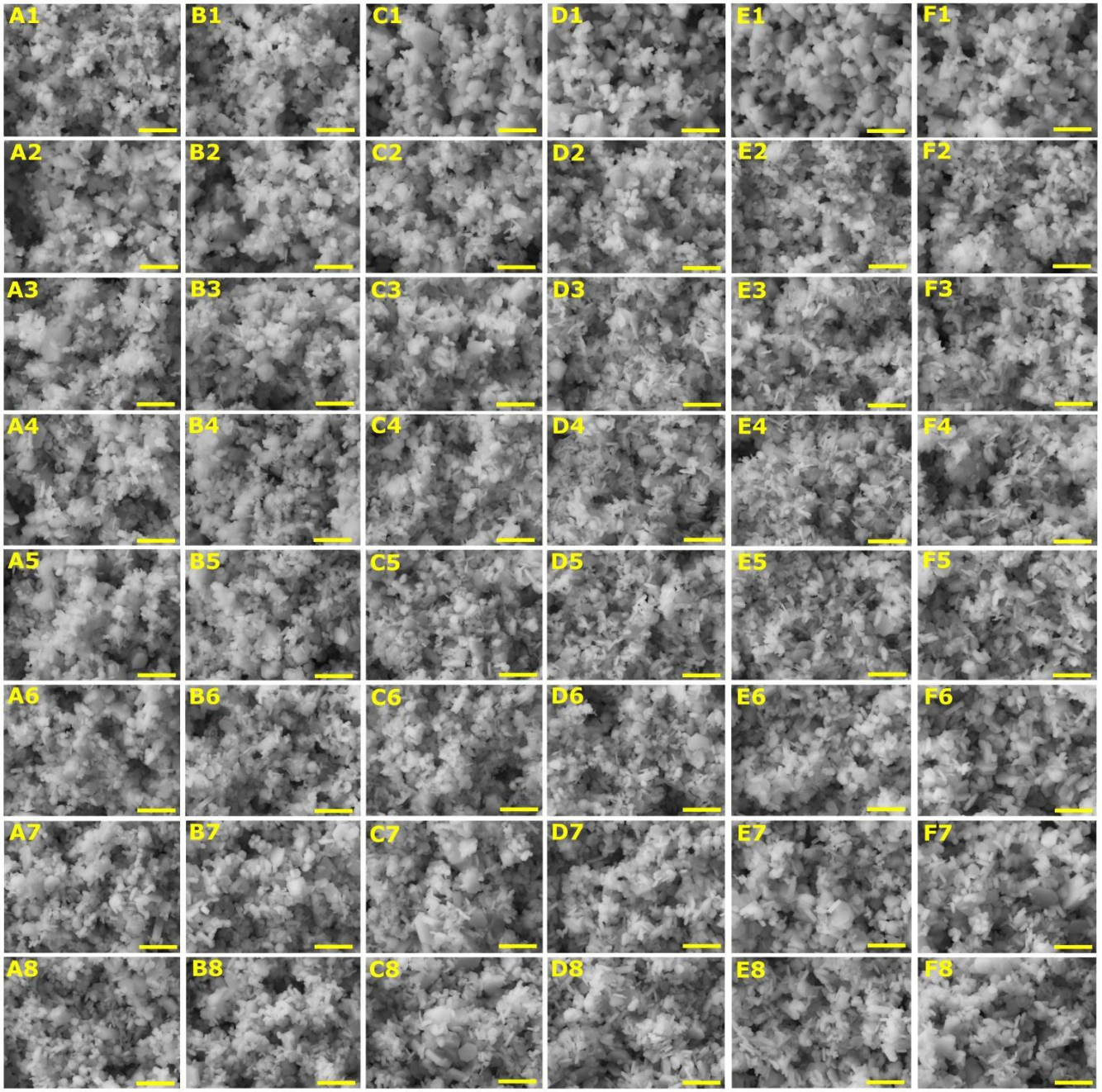

Figure S9. Overview of SEM images of $Cs_3Bi_2(Cl,Br,I)_9$ double salt samples in the plate presented in Fig. S7a. Scale bar is 2.5 μm.

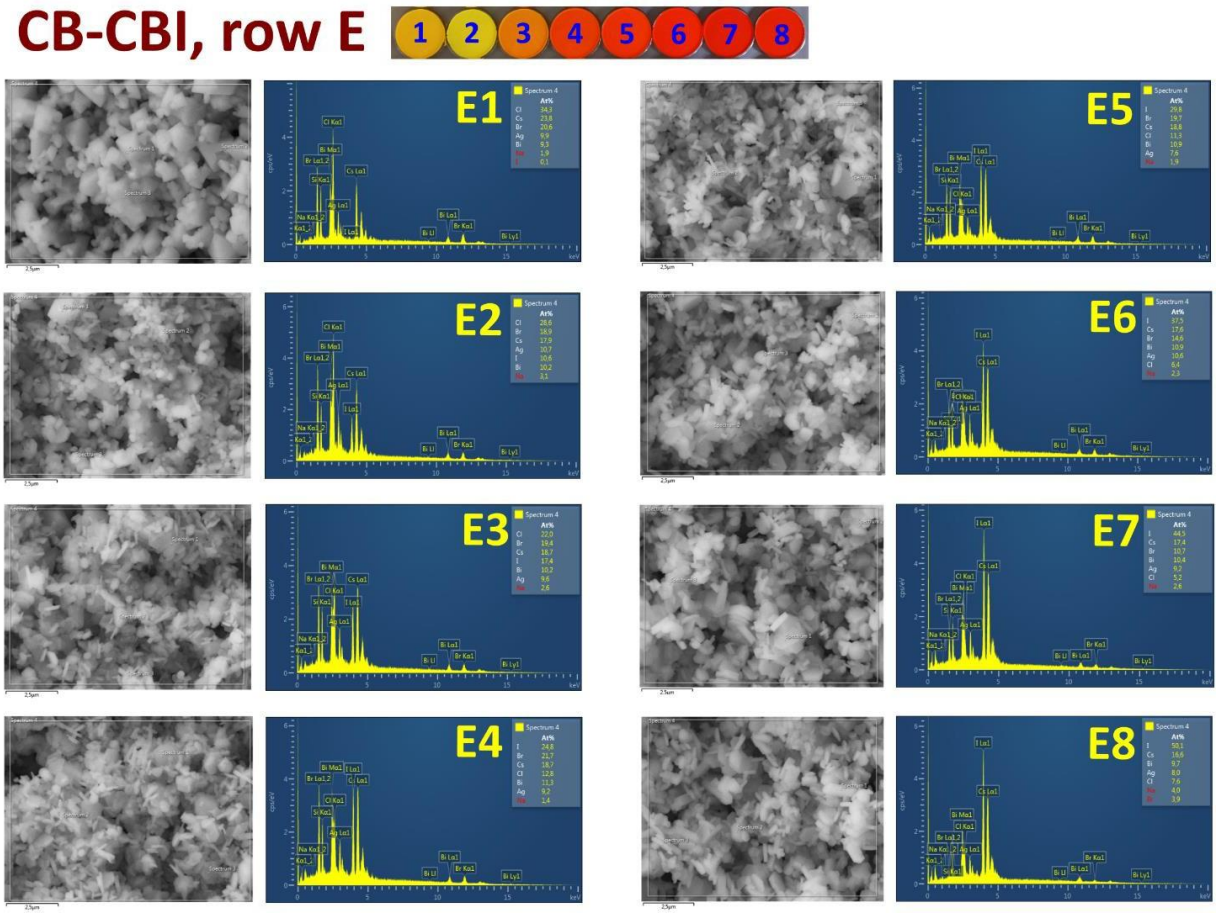

Figure S10. Exemplary EDX spectra of the CB-CBI sample array collected for E1-E2 samples. SEM images in the left panel show the area for which the EDX spectra (right panel) were collected. The presented EDX spectra correspond to the entire probed area (spectrum 4 in the SEM images).

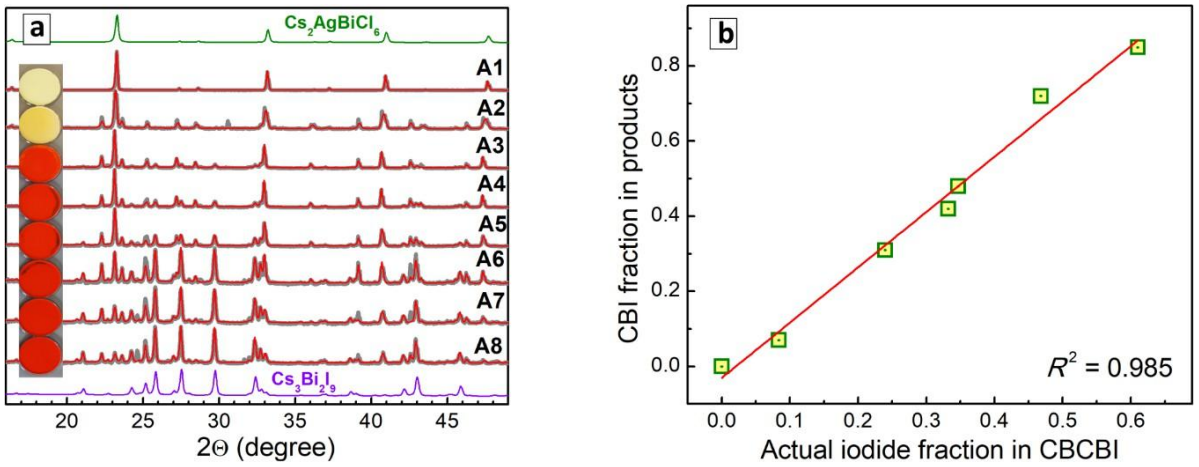

Figure S11. Overview of the characteristics of samples produced from $Cs_2AgBiCl_6$ by anion exchange solely with NaI (series Ax): (a) powder XRD patterns; (b) dependence of the fraction of $Cs_3Bi_2I_9$ double salt on the actual iodide fraction determined by EDX. The content of the CBI phase was evaluated by the Rietveld refinement of the experimental XRD profiles using a combination of CBB and CABC reference structures.

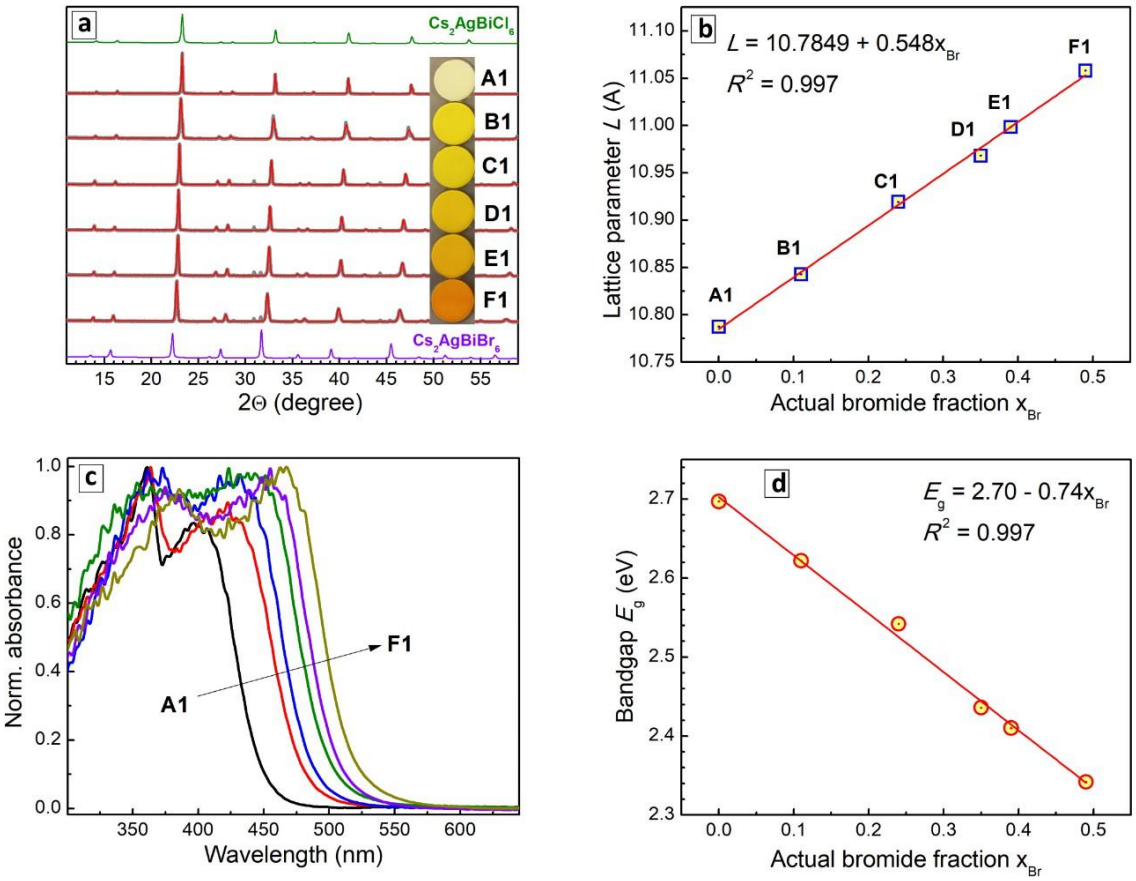

Figure S12. Overview of the characteristics of $Cs_2AgBi(Cl,Br)_6$ double perovskites produced by anion exchange with NaBr (series x1): (a, c) powder XRD patterns (a) and absorption spectra (c); (b,d) dependences of lattice parameter (b) and bandgap (d) on the actual bromide fraction.

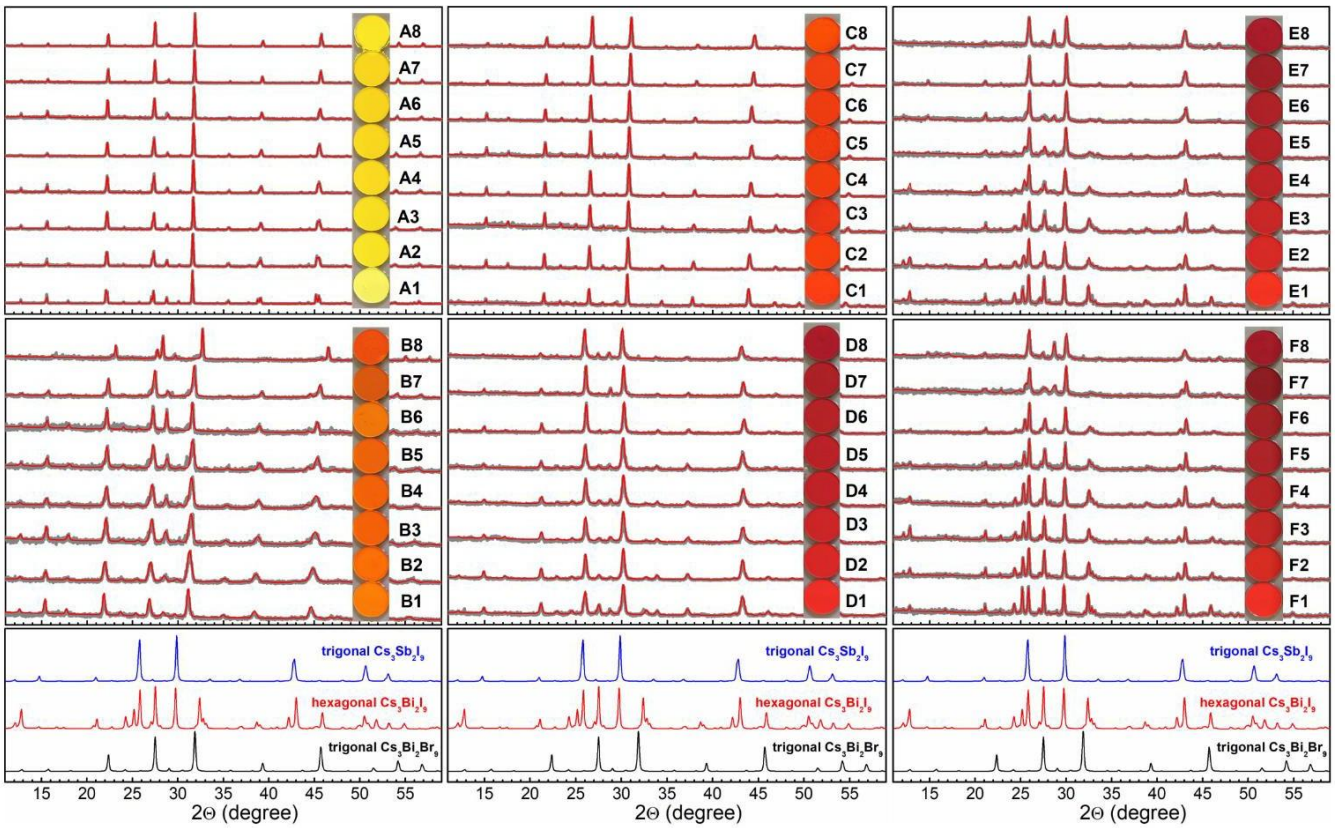

Figure S13. The collection of powder XRD patterns of all samples in the anion-exchanged sample array produced from $Cs_3(Bi,Sb)_2Br_9$: gray lines are experimental data, red lines represent Rietveld refinement, lower panels show reference patterns used for the Rietveld refinement.

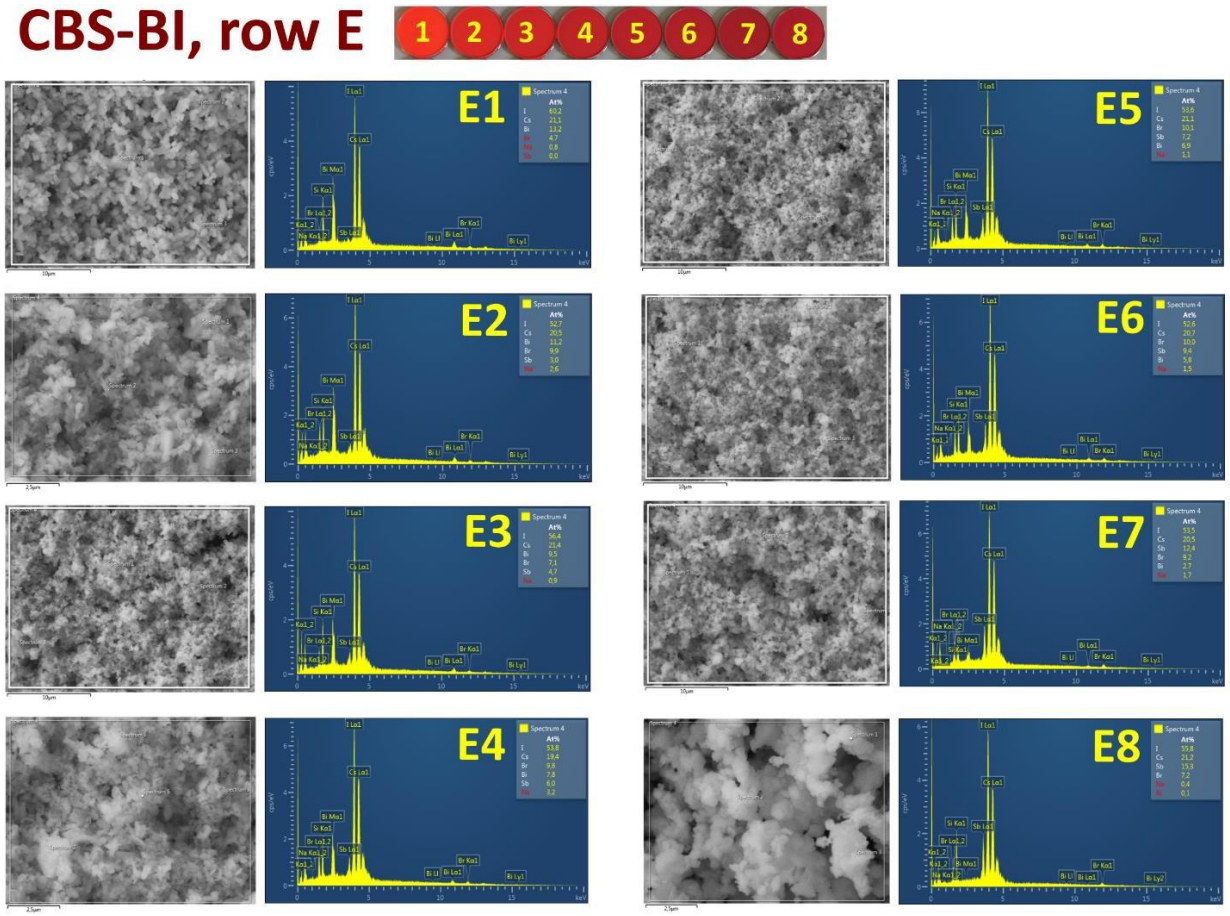

Figure S14. Exemplary EDX spectra of the CBS-BI sample array collected for E1-E2 samples. SEM images in the left panel show the area for which the EDX spectra (right panel) were collected. The presented EDX spectra correspond to the entire probed area (spectrum 4 in the SEM images).

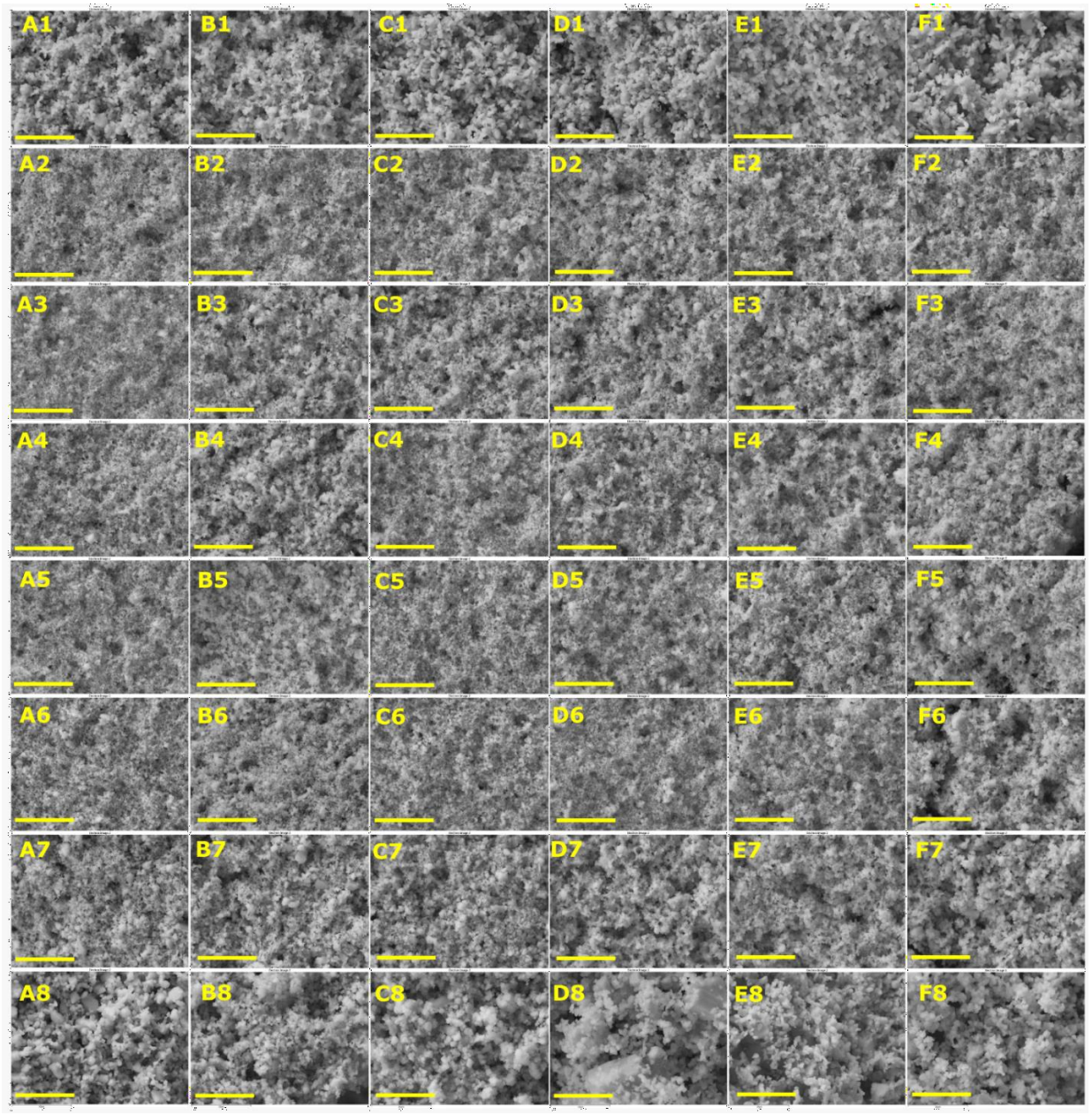

Figure S15. Overview of SEM images of CBS-BI double salt samples. Scale bar is 10 µm.

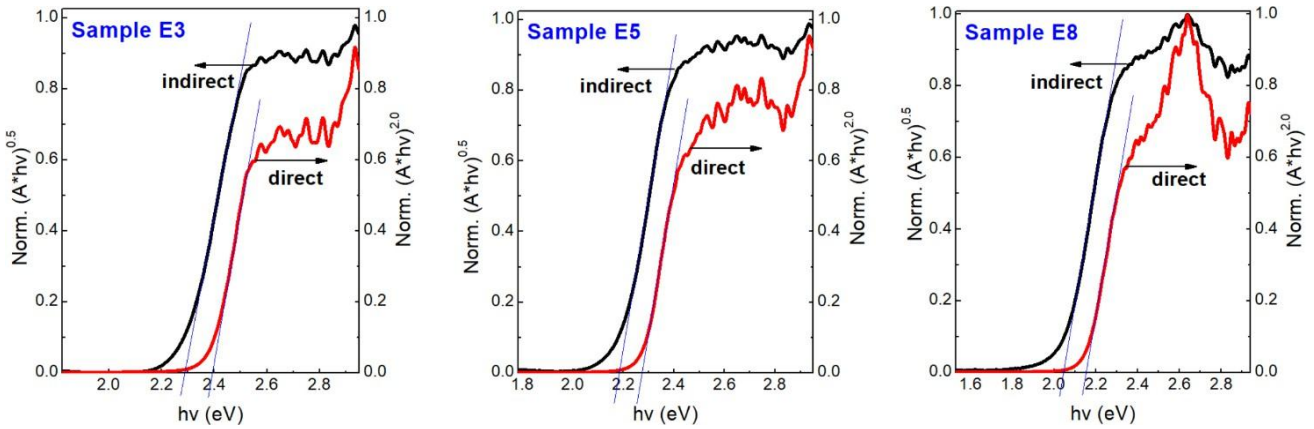

Figure S16. Normalized absorption spectra of selected CB-CBI samples E3, E5, and E8 in coordinates of the Tauc equation for indirect (black curves) and direct (red curves) interband electronic transitions. Blue curves show tangents to the absorption slopes.

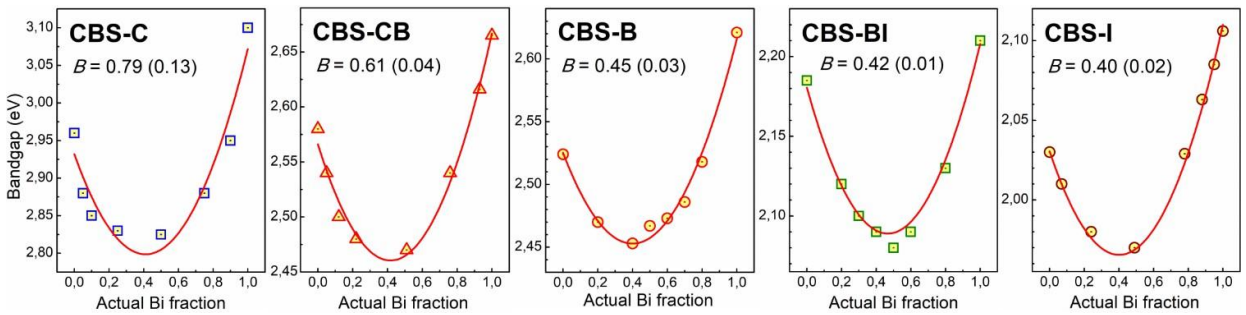

Figure S17. Bandgap dependences for different CBS-X double salts (scatters) with corresponding fitting (solid lines) using the equation presented in the main text.